Proc. Nat. Acad. Sci. USA
Vol. 69, No. 12, pp. 3746–3750, December 1972

The Three-Dimensional Structure of Yeast Phenylalanine Transfer RNA: Shape of the Molecule at 5.5-Å Resolution

(x-ray diffraction/isomorphous/Os/Sm/Pt)

S. H. KIM*, G. QUIGLEY, F. L. SUDDATH, A. McPHERSON, D. SNEDEN, J. J. KIM, J. WEINZIERL, P. BLATTMANN, AND ALEXANDER RICH

Department of Biology, Massachusetts Institute of Technology, Cambridge, Mass. 02139

Contributed by Alexander Rich, October 12, 1972

ABSTRACT **Three isomorphous heavy-atom derivatives have been obtained of orthorhombic crystals of phenylalanine transfer RNA from yeast. These derivatives contain osmium, samarium, and platinum. The positions of the heavy atoms have been determined; these have been used to calculate a three-dimensional electron-density map of transfer RNA at a resolution of 5.5 Å. The map shows a high contrast between the molecular boundaries and the solvent areas, so that most of the external shape of the molecule can be determined. The molecule appears to be 92Å long and to have a width varying from 16 Å to 34 Å. There are some narrow regions in the molecule that connect more globular regions. The electron density map shows chains of dense objects approximately 6 Å apart that are probably due to adjacent phosphate groups on the polynucleotide chain. At the present stage of the analysis it is not possible to trace the entire backbone unambiguously; however, the data at this resolution suggest no apparent similarity between the folding of the molecule and any of the tertiary structure models proposed for transfer RNA.**

Transfer RNA (tRNA) molecules play a central role in the assembly of amino acids into polypeptide chains. Similarities in the nucleotide sequence of different tRNAs suggest that they have common features of secondary, and even tertiary, structure (1). Although tRNA molecules crystallize readily, it has been difficult to obtain crystals with a sufficiently high resolution to make them useful for extensive x-ray diffraction analysis. A year and a half ago we reported that it was possible to obtain orthorhombic crystals of yeast phenylalanine tRNA that yielded x-ray diffraction patterns with a resolution of 2.3 Å (2). We have continued to work on the analysis of this crystalline form; here, we report on the preparation and analysis of three isomorphous derivatives containing osmium, platinum, and samarium. Using the method of isomorphous replacement, we have calculated a three-dimensional electron-density map of tRNA at a resolution of 5.5 Å. This electron density map shows a very high contrast between the molecule and the solvent in the crystal. This contrast allows us to detect the overall shape of tRNA over most of its molecular boundary. In addition, some portions of the ribophosphate chain can be visualized, although it is not possible to trace the chain unambiguously at the present resolution.

METHODS

The orthorhombic crystals of yeast phenylalanine tRNA (Boehringer–Mannheim) were prepared (2) with magnesium and spermine as cations. Crystals were mounted in sealed capillaries, together with a small volume of mother liquor. X-ray diffraction photographs were taken with CuK_α radiation on an Elliott rotating-anode x-ray generator. Heavy atom derivatives were obtained by adding compounds containing the heavy atom to the mother liquor and allowing them to diffuse into the crystal. The presence of the heavy atoms was detected by changes in the diffraction intensity monitored on films. Large crystals of the same type were then mounted for three-dimensional data collection on a Picker FACS I diffractometer. Data were collected by use of an omega step scan in a series of six concentric shells out to a resolution of 5.5 Å, each shell contained 200 independent reflections. A set of 12 standard reflections was monitored periodically for indications of crystal degradation. When the average intensity of the monitored reflections decreased 10–15%, the crystal was discarded and a new specimen was mounted.

The preparation of an osmium derivative of yeast formylmethionine tRNA has been reported (3). In our work we have prepared an ATP–osmate bipyridine ester to be used in forming heavy atom derivatives. It was prepared by use of the procedure for forming osmate bipyridine esters of nucleosides (4). The sodium salt of ATP (Sigma) was reacted with $OsO_3(pyridine)_2$ in water–pyridine solution (2:1 v/v), and the reaction was followed by thin layer chromatography on Merck Cellulose F plates in isopropanol–17 N NH_4OH–H_2O 50:1:49. The ATP–Os ester gave a visible grey-brown spot on the chromatogram. To complete the conversion of ATP into the Osmate ester, an excess of OsO_3py_2 was required. The brown product was isolated by evaporation of the solvents.

RESULTS

Addition of the osmium–ATP complex to the mother liquor produced noticeable changes in the diffraction pattern. The three-dimensional Patterson function was interpreted to indicate one osmium position, which was then refined in projection by the use of standard least-squares procedures.

Significant differences in diffraction patterns had been noted with crystals soaked with platinum tetrachloride and, to a lesser extent, with crystals soaked with samarium acetate. Initial difference Patterson maps of these derivatives were not interpretable; however, a cross Fourier synthesis based on the osmium data revealed two Sm sites which were subsequently refined. A similar analysis of the $PtCl_4$ data revealed the presence of three platinum sites which were also refined. Three-dimensinal electron-density maps were calculated with the combined phase data from the Os, Sm, and Pt derivatives (5).

* Present address: Dept. of Biochemistry, Duke University, Durham, N.C. 27707.

The orthorhombic unit cell is in space group $P2_12_12_1$ with $a = 33$ Å, $b = 56$ Å, $c = 161$ Å. The coordinates and relative occupancies of the heavy atom sites are listed in Table 1, where we assume an occupancy of 1.0 for the osmium derivative. Based on this criterion, the two samarium sites have occupancies of 0.5 and 0.6. The three platinum sites, as shown in Table 1, had occupancies of 0.9 and 0.8 for two of the sites and 0.6 for the third. Diffraction data were collected to a resolution of 5.5 Å (1200 independent reflections) for the native crystal and its three derivatives. Table 2 lists the refinement statistics of the various derivatives. The osmium–ATP derivative has the highest degree of reliability. All of these have been combined to compute a "best" three-dimensional electron density map at a resolution of 5.5 Å (5). The electron density map was calculated in increments of 0.05, 0.025, and 0.01 along x, y, and z, giving approximately 1.5 Å separation between points in all directions. Two maps were then drawn sectioned along a and along b.

TABLE 1. *Heavy atom positions*

Heavy atom	x	y	z	Relative occupancy*
ATP–Os	0.0237(19)	0.1942(10)	0.0658(3)	1.0
Sm-1	0.5574(25)	0.1634(15)	0.2773(5)	0.5
Sm-2	0.2779(33)	0.3726(19)	0.2312(6)	0.6
Pt-1	0.0703(29)	0.2392(16)	0.3239(5)	0.9
Pt-2	0.0077(28)	0.1884(15)	0.0562(5)	0.8
Pt-3	0.2391(65)	0.4434(34)	0.1125(11)	0.6

The estimated standard deviations in parentheses refer to the last digits.

* Based on the assumed occupancy of 1.0 for the osmium derivative.

The electron density map has several unusual features. Fig. 1 shows a view along the a axis through the entire unit cell. This projection shows two molecules lying one above another in antiparallel orientation with the c axis horizontal. The contrast between solvent regions and the tRNA molecule in this projection is striking. There are two horizontal dense regions in the projection that are surrounded by large open spaces occupied by solvent. The crystals contain 70% water (6), the bulk of which is present in large, open channels that pass through the entire crystal. In Fig. 1 the dashed line represents the envelope of one molecule as viewed along the a axis.

All of the heavy atom sites in the molecule appear to be accessible to the solvent in the crystal. We do not know why both samarium sites and one of the platinum sites have lower occupancy than that of the osmium site. The lower samarium

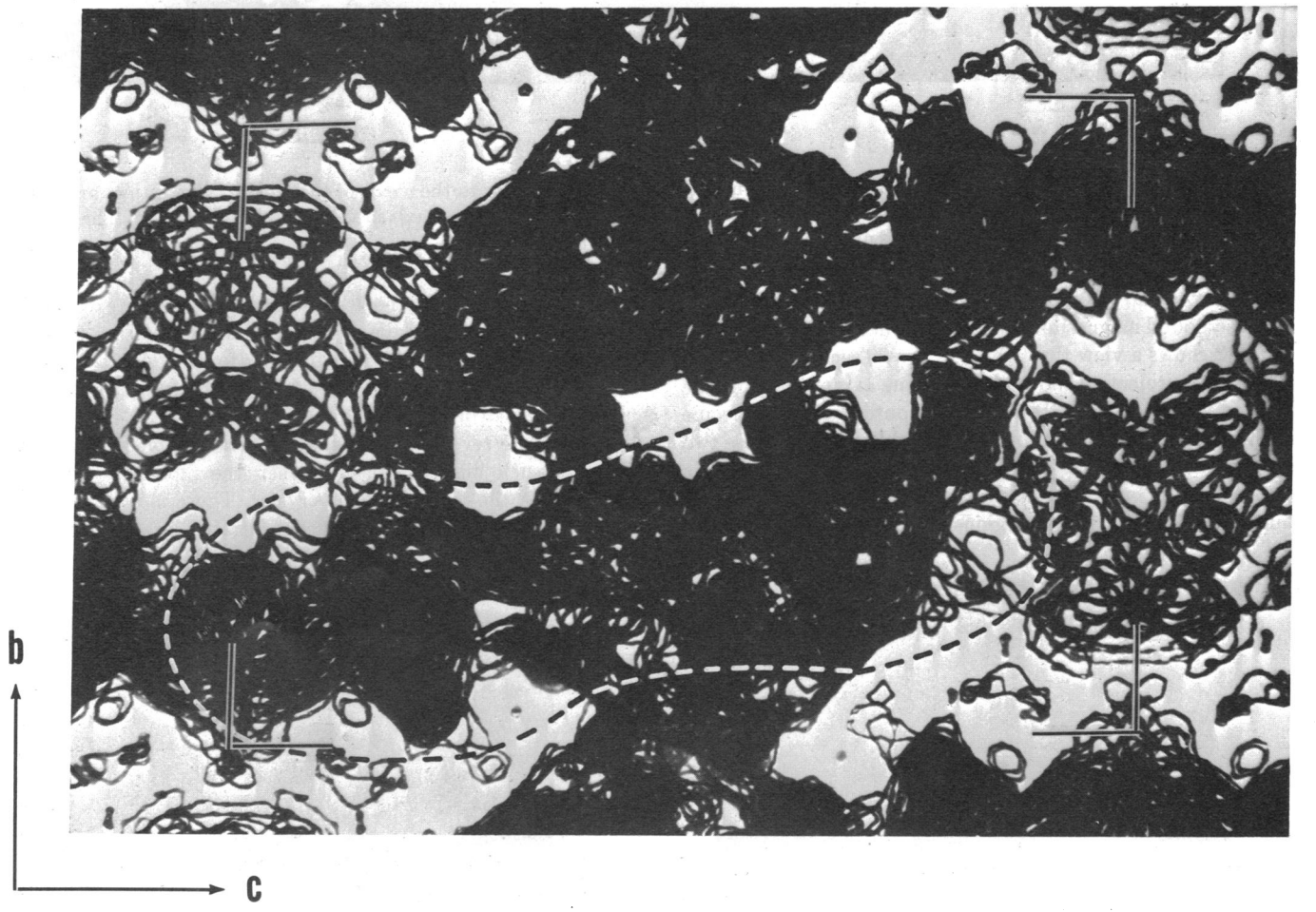

FIG. 1. A view of the entire three-dimensional electron-density map of yeast phenylalanine tRNA as seen down the a axis. The map is computed in 20 sections 1.65-Å apart along the a axis. Contours are plotted at arbitrary heights. The areas with low electron density contain solvent. The *dashed line* shows the outline of one molecule. The *corner brackets* include the entire b axis and one-half of the c axis.

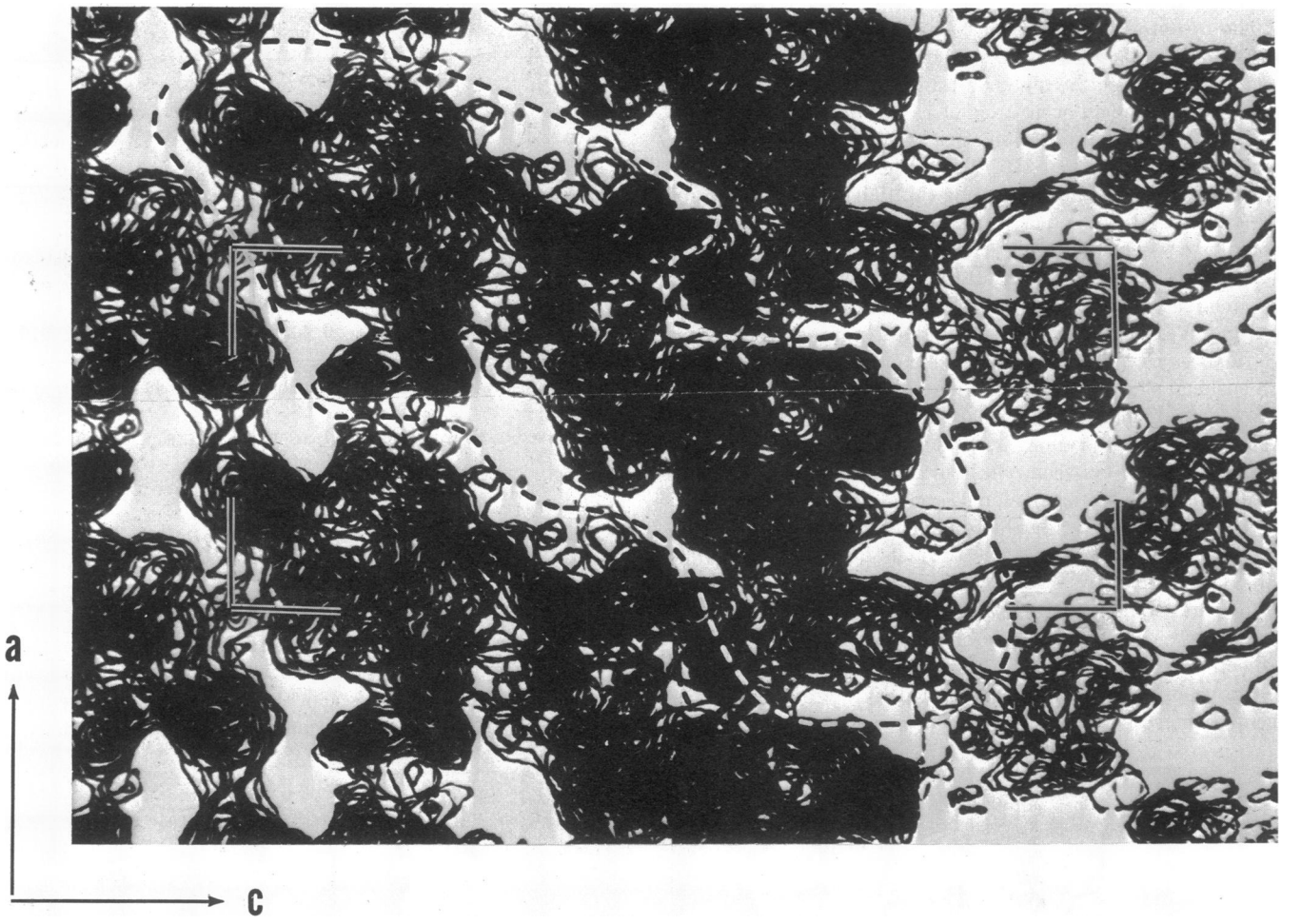

FIG. 2. A view through 18 of the 20 sections in the asymmetric unit perpendicular to the *b* axis of the crystal. The sections are 1.4-Å apart. The *corner brackets* include the entire *a* axis in the vertical direction and half of the *c* axis in the horizontal direction. The *dashed line* represents the outline of one tRNA molecule.

occupancy could be explained if the samarium ions have replaced bound magnesium ions in the structure.

Fig. 2 shows a view through 18 of the 20 sections along the *b* axis. This projection shows that the long axis of the molecule is tilted with respect to the *c* axis. The outline of the molecule in this projection is shown by the dashed line. From these two projections it can be seen that the molecule does not have a smooth shape, but rather has an irregular outline, with thick bulges connected by thin regions. The separation between the molecules along the *b* axis can be seen more easily if viewed through a smaller number of sections. Fig. 3 shows a projection along the *a* axis through four levels of the electron density map. In these sections the molecular outline is resonably well defined.

There are several factors that may be responsible for producing such high contrast between the molecules and the solvent in the transfer RNA crystal. There is a high water content, and it appears to be concentrated largely in the in-

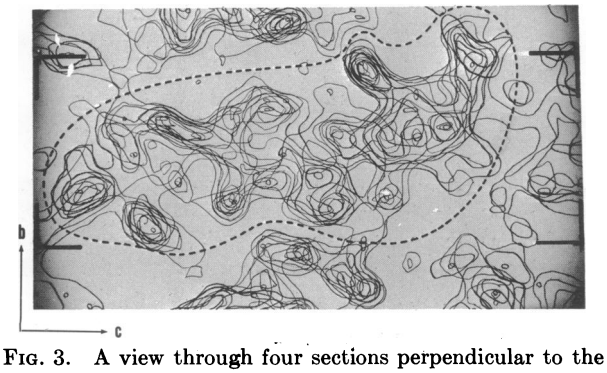

FIG. 3. A view through four sections perpendicular to the *a* axis. The *dashed line* shows the separation between one molecule and its neighbors. The corner brackets include half of the *b* axis and half of the *c* axis.

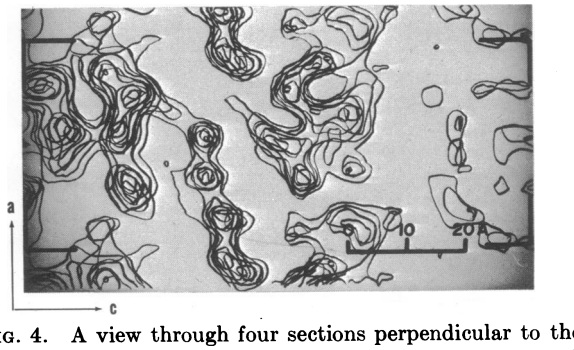

FIG. 4. A view through four sections perpendicular to the *b* axis. A chain of connected electron-dense centers is shown passing near the center of the field. The *brackets* include the entire *a* axis and half of the *c* axis.

TABLE 2. *Refinement statistics*

	Spacing (Å)	21.74	14.49	10.87	8.70	7.25	6.21	5.43	Average (total)
A. Total Data	mean m	.627	.768	.724	.783	.700	.696	.560	.672
	mean $\|F_N\|$	2028	1086	905	675	538	494	506	616
	mean $\|F_C\|$	2147	1105	872	631	499	446	511	665
	R Modulus	1.140	.693	.672	.476	.566	.597	.713	.627
	R Weighted	1.172	.540	.618	.298	.456	.522	.827	.546
B. Derivatives									
(*a*) ATP-Os	RMS closure	169	116	143	82	92	91	105	
	RMS f	191	212	189	188	174	172	156	
	RMS Error	99	21	24	25	28	33	40	
All data	R Modulus	.937	.497	.539	.383	.419	.401	.453	.442
	R Weighted	.652	.311	.570	.195	.267	.270	.424	.318
	Number of reflexions	20	52	87	150	207	282	333	(1131)
Centric data	R Modulus	.937	.557	.633	.514	.631	.573	.770	.631
	Number of reflexions	16	31	44	59	70	87	89	(396)
(*b*) Sm	RMS closure	151	101	84	80	70	87	107	
	RMS f	103	123	130	114	115	110	99	
	RMS Error	98	17	19	19	22	26	29	
All data	R Modulus	1.092	.800	.599	.631	.477	.640	.864	.679
	R Weighted	1.282	.687	.423	.482	.368	.628	1.141	.644
	Number of reflexions	20	52	86	150	207	278	329	(1122)
Centric data	R Modulus	1.211	1.046	.742	.911	.795	.811	1.097	.903
	Number of reflexions	16	31	43	59	70	87	85	(391)
(*c*) Pt	RMS closure	387	257	246	145	213	200	260	
	RMS f	290	282	277	259	250	228	230	
	RMS Error	99	25	28	32	40	53	72	
All data	R Modulus	1.292	.798	.795	.474	.710	.727	.826	.736
	R Weighted	1.875	.758	.777	.324	.709	.773	1.184	.747
	Number of reflexions	20	52	87	150	206	282	332	(1129)
Centric data	R Modulus	1.166	.939	.833	.594	.905	.831	1.085	.883
	Number of reflexions	16	31	44	59	69	87	88	(394)

n, number of terms; m, figure of merit; f_H, calculated structure factor of heavy atom alone; F_N, structure factor of native crystal; F_{NH}, structure factor of heavy-atom derivative crystal; F_C, centric structure factor of native crystal.

RMS Closure = $(\Sigma(|F_{NH}| - |F_N + f_H|)^2/n)^{1/2}$

RMS f = $(\Sigma|f_H|^2/n)^{1/2}$.

RMS Error (F_{NH}) = estimated experiental error in F_{NH}.

R Modulus = $\Sigma||F_{NH}| - |F_N + f_H||/\Sigma|f_H|$.

R Weighted = $\Sigma w(|F_{NH}| - |F_N + f_H|)^2/\Sigma w|f_H|^2$.

termolecular regions that form large aqueous channels which go through the crystal. There are some contacts between the molecules, but they are few in number. This sparsity may reflect the polyanionic character of the tRNA molecule, in that the molecules are all highly charged. Furthermore, the solvent has a relatively low electron density as compared to the ammonium sulfate solutions that are often used in macromolecule crystallization. Finally, the transfer RNA molecule has a phosphate group as part of each nucleotide. The phosphate group has a total of 48 electrons, and it appears as an electron-dense region even at a resolution of 5.5 Å. A similar contrast is usually not visible in the electron density map of a protein at a comparable resolution because of the absence of systematic groups along the backbone that have a large number of electrons.

In several places in the electron density map there is a series of connected peaks that suggest a ribose phosphate backbone. An example of this is seen in Fig. 4, which shows four adjacent sections along the y axis. Several electron dence areas with a separation of approximately 6 Å can be seen forming an elongated chain.

It is of interest that portions of the molecule show well-defined loops. One of these which appears to be on the outside of the molecule is shown in Fig. 5. This loop has a diameter of 17 Å and contains seven electron-dense regions, six of which are visible in Fig. 5.

We have constructed a solid three-dimensional model of the electron density map from which one can obtain an overall impression of the molecular shape (Fig. 6). It is seen to be oblong, with an overall length of approximately 92 Å. Along the b axis the molecule has a width that varies from 16 Å at its narrowest point to 32 Å at its widest. It can be seen

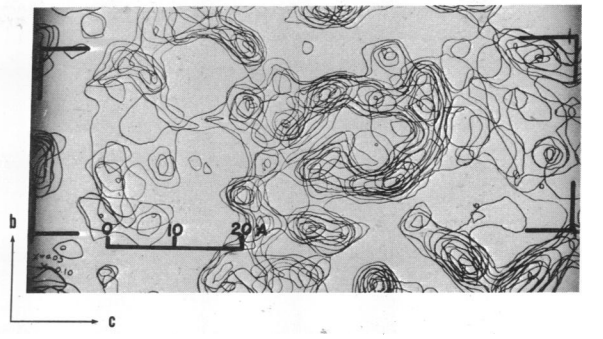

FIG. 5. A view of three sections perpendicular to the a axis. A loop in the molecule is shown. The corner brackets include half of the b axis and half of the c axis.

that the molecule is quite irregular in outline and has a number of protuberances that are visible at this resolution. There are several elongated masses of electron-dense matter that are seen to come out of the molecule and re-enter in a manner that suggests that they may represent loops in the ribose phosphate backbone of the polynucleotide chain.

Significant portions of the polynucleotide backbone can be traced at the present resolution; however, it is impossible to trace the entire chain unambiguously. At several points in the molecule, electron-dense regions merge together in a way that yields several alternative choices for chain tracing. The total number of ambiguous points is large enough that we cannot make a clearcut decision about the tertiary structure of the molecule at the present resolution. However, since we have used less than 20% of the data that we can obtain, the present results lead us to expect that a full tracing of the polynucleotide backbone will be possible from further analysis at higher resolution.

DISCUSSION

The overall dimensions of the transfer RNA molecule are similar, although slightly larger than those that we had initially estimated from an analysis of the three-dimensional Patterson function for *Escherichia coli* formylmethionine tRNA (7). There are two globular regions of the molecule, which are connected by a thinner neck region. This finding suggests that the two globular regions may be able to move independently of each other, thereby producing unusual dynamic characteristics. This configuration also suggests that cleavage in the neck region might liberate a portion of the molecule that would retain its three-dimensional folding.

Even at the present resolution, several features of the molecule shown in Fig. 6 suggest various biochemical functions. We will defer a discussion of these until the higher-resolution data are available.

One of the unusual features associated with the orthorhombic crystals of yeast phenylalanine transfer RNA is the fact that the unit cell undergoes an unusual set of shrinkage stages when the crystal is partially dried (6). In these transformations the a and the b axes change very little, but the c axis changes abruptly from 161 Å to 128 Å, and then finally to 109 Å. However, the distribution of diffraction intensity does not change substantially during these transformations. Figs. 1 and 2 suggest an interpretation of this shrinkage phenomenon. The molecular packing along the a and the b axes is very close, but along the c axis there is a large, low-density region found between the molecules. It is possible that this region may be occupied by the polycationic spermine

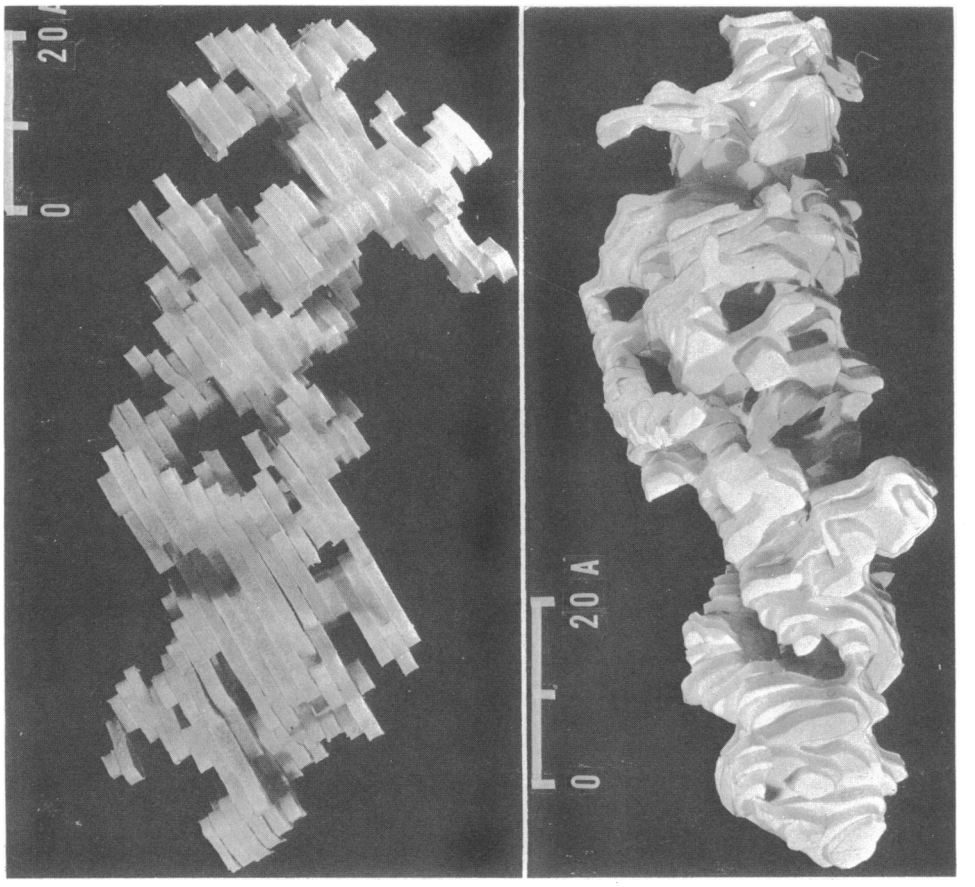

FIG. 6. Photographs of the 5.5-Å resolution model of yeast phenylalanine tRNA. (*left*) View approximately along the *b* axis. (*right*). View at right angle to the other view.

molecules which are necessary in order to form the high-resolution orthorhombic crystal. These molecules are flexible and could undergo considerable changes in configuration during the shortening of the *c* axis. Alternatively, it is possible that some portion of the polynucleotide chain extends into this region but is not held in a completely rigid configuration. If this were so, such a region would have a significantly larger temperature factor and the effective electron density would be reduced.

At the present resolution we are confronted by several ambiguities. As mentioned above, one of these concerns the tracing of the polynucleotide backbone. Another concerns the detailed separation between the molecules at one or two points. There is very dense packing along the *a* axis, and some regions of the molecule come in close contact with adjoining neighbors. Since the molecules have the same negative charge, it is possible that intermolecular contacts are stabilized by the presence of magnesium ions. If this were the case, it would give rise to an additional electron dense region and make it difficult to determine the exact boundary between the molecules. Although we are reasonably confident about most of the outlines of the molecule shown in the model (Fig. 6), some of the protuberances attached to one side of the molecule may in fact be found on exactly the opposite side. We hope that these ambiguities will be resolved by a further analysis of the structure at higher resolution.

Several transfer RNA molecules have been sequenced; all of the sequences are consistent with the "cloverleaf" model of secondary structure, in which there are stems and loops (1). Several features of the molecule at the present resolution are consistent with the existence of small helical segments and loops. Many models of the tertiary structure of tRNA have been proposed, most of which use the cloverleaf secondary structure. Although it is too early in the analysis to make a firm statement, it is our impression that none of the proposed tertiary structure models are consistent with the form of the molecule that we see at this resolution.

We are grateful to the following individuals and the members of their laboratories: Drs. W. N. Lipscomb and K. Ericks for film scanning assistance and Drs. V. Day, E. Hazen, M. G. Rossman, P. G. Lenhert, and J. M. Rosenberg for computer programs and assistance. This research was supported by grants from the National Institutes of Health, the National Science Foundation, the National Aeronautics and Space Administration, and the American Cancer Society. G. Q. is a postdoctoral fellow of the National Institutes of Health; A. M. and F. L. S. are postdoctoral fellows of the American Cancer Society; D. S. and J. W. are supported by a National Institutes of Health Training Grant.

1. For a review see Cramer, F. (1971) *Progr. Nucl. Acid Res. Mol. Biol.* **11**, 391–421.
2. Kim, S. H., Quigley, G., Suddath, F. L. & Rich, A. (1971) *Proc. Nat. Acad. Sci USA* **68**, 841–845.
3. Schevitz, R. W., Navia, M. A., Bantz, D. A., Cornick, G., Rosa, J. J., Rosa, M. D. H. & Sigler, P. B. (1972) *Science* **177**, 429–431.
4. Subbaraman, L. R., Subbaraman, J. & Behrman, E. J. (1971) *Bioinorg. Chem.*, **1**, 35–55.
5. Blow, D. M. & Crick, F. H. C. (1959) *Acta Crystallogr.* **12**, 794–802.
6. Kim, S. H., Quigley, G., Suddath, F. L., McPherson, A., Sneden, D., Kim, J. J., Weinzierl, J. & Rich, A. (1972) *J. Mol. Biol.*, in press.
7. Kim, S. H. & Rich, A. (1969) *Science* **166**, 1621–1624.